Check for updates

This article can be cited before page numbers have been issued, to do this please use: Z. He, A. Korre, G. H. Kelsall, Z. Nie and M. Colet-Lagrille, *RSC Sustain.*, 2024, DOI: 10.1039/D4SU00223G.

ROYAL SOCIETY OF CHEMISTRY

Sustainability spotlight

The global necessity to decarbonise energy storage and conversion systems is causing rapidly growing demand for lithium-ion batteries, so requiring sustainable processes for lithium carbonate (Li_2CO_3) production.

We established a comprehensive life cycle inventory to evaluate environmental impacts of its production by evaporation of Atacama brines, analysing effects of brine composition, water supply, evaporation rates, waste management and chemical processes deployed. Results highlight significant environmental and water resource impacts, emphasising the urgency of transitioning to water-saving and more energy efficient processes in arid regions and the importance of site-specific information for accurate emissions and environmental impacts assessment.

Identifying and evaluating the impacts of Li_2CO_3 production is essential for developing materials utilisation strategies aligned with United Nations sustainable development goals (SDG 6,7,9,13 and 15).

RSC Sustainability Accepted Manuscript

ARTICLE

Environmental and Life Cycle Assessment of Lithium Carbonate Production from Chilean Atacama Brines

Zijing He [a], Anna Korre *[ab], Geoff Kelsall [c], Zhenggang Nie [a] and Melanie Colet Lagrille [d]

The exponentially growing market for lithium-ion batteries (LIBs) is driving the development of more environmentally benign processes for producing lithium carbonate, a key precursor. Extracting lithium(I) from brine is a cost-effective method, particularly in the Lithium Triangle in South America, including the Atacama Desert in Chile. Life cycle assessment (LCA) was used to assess the environmental impacts of lithium(I) production by establishing a comprehensive life cycle inventory (LCI) with data from modelling, literature, technical reports and the Ecoinvent database. Information about evaporation rates from Atacama salars, the performance of the northern Chile electrical grid fuel mix and present waste management processes were analysed to establish the water balance, water footprint (WF), water scarcity footprint (WSF) and to estimate in Aspen Plus and Sphera the environmental performance of the battery-grade lithium carbonate production process. The results predicted significant environmental impacts associated with production of input chemicals such as sodium hydroxide (NaOH) and sodium carbonate (Na_2CO_3), as well as with energy conversion from the carbon intensive electrical supply in northern Chile. The waste dumps and surface impoundments required for the production process did not result in significant leachate infiltration, although considerable land areas are occupied. The modelling and analysis results highlighted the importance of accurate brine evaporation rates on the process water balance estimation and on the conventional manufacturing process emissions; insufficient evaporation rates increased the water footprint of chemical production processes. The water resource stress in the arid Atacama region was evident from predicted water balances, WFs and WSFs, emphasising the necessity to innovate less time-consuming and water-conserving processes to increase sustainability.

1. Introduction

Demand for lithium(I) compounds is growing rapidly, driven by the global necessity to decarbonise chemical-to-electrical energy conversion with renewable energy systems, addressing their intermittency and balancing electrical power supply and demand by energy storage, inter alia in lithium batteries. Fig. 1 shows the global lithium(I) consumption and the proportion of its use in batteries, with global lithium(I) consumption reaching 180 kt a^{-1} in 2023.[1] Although affected by the global COVID-19 pandemic, demand decreased in the first half year of 2020, but the lithium-ion battery market recovered its strong growth in the second half year, as the global economy started to recover. Between 2020 and 2022, lithium(I) mining output expanded by ca. 80 %, despite which market demand for lithium(I) remains tight, resulting in the lithium(I) market price increasing more than five-fold over this period.[2] However, annual average U.S. lithium carbonate prices in 2023 decreased by 32 % from that in 2022, mainly due to policy issues, especially relations with China, and slower growth in demand.[1,3] The instability of the lithium(I) market has emphasised the significance of cost-effective, dependable and robust supply chains, particularly for countries that prioritise affordability and those undergoing rapid energy transitions. Lithium(I) can be extracted primarily from hard-rock ores, such as spodumene, petalite and lepidolite, and brines. Australia is the world's leading producer of lithium(I), relying primarily on spodumene, whereas Chile is the second largest producer country, relying on Li^I-rich brine resources found in high altitude desert salars.[4,5] Interestingly, lithium(I)-containing brines are mostly concentrated in the so-called Lithium Triangle of South America.[6] Extracting lithium(I) from hard rock ores requires various processes, which are complex, energy-intensive and may include several chemical transformations. Due to lower production costs, brine is a more common source of lithium(I), which in principle may be extracted from salt lake brines, geothermal brines and even seawater. However, lithium(I) extraction from geothermal brine has not been commercialised on a large scale, being only at the pre-commercial demonstration stage.[2] As yet, there are no cost-effective processes to extract lithium(I) from seawater, typically at concentrations of 0.1- 0.2 ppm,[7,8] whereas lithium(I) concentrations of 200 - 700 ppm in most salt lake brines are considered as commercially attractive.[9]

[a.] Department of Earth Science and Engineering, Imperial College London, Exhibition Road, SW7 2AZ, London, United Kingdom. E-mail: Zijing.he21@imperial.ac.uk; a.korre@imperial.ac.uk
[b.] Energy Futures Lab Imperial College London, Exhibition Road, SW7 2AZ, London, United Kingdom.
[c.] Department of Chemical Engineering, Imperial College London, Exhibition Road, SW7 2AZ, London, United Kingdom.
[d.] Department of Chemical Engineering, University of Chile, Av. Beauchef 851, 8370458 Santiago, Región Metropolitana, Chile.
Electronic Supplementary Information (ESI) available: [details of any supplementary information available should be included here]. See DOI: 10.1039/x0xx00000x
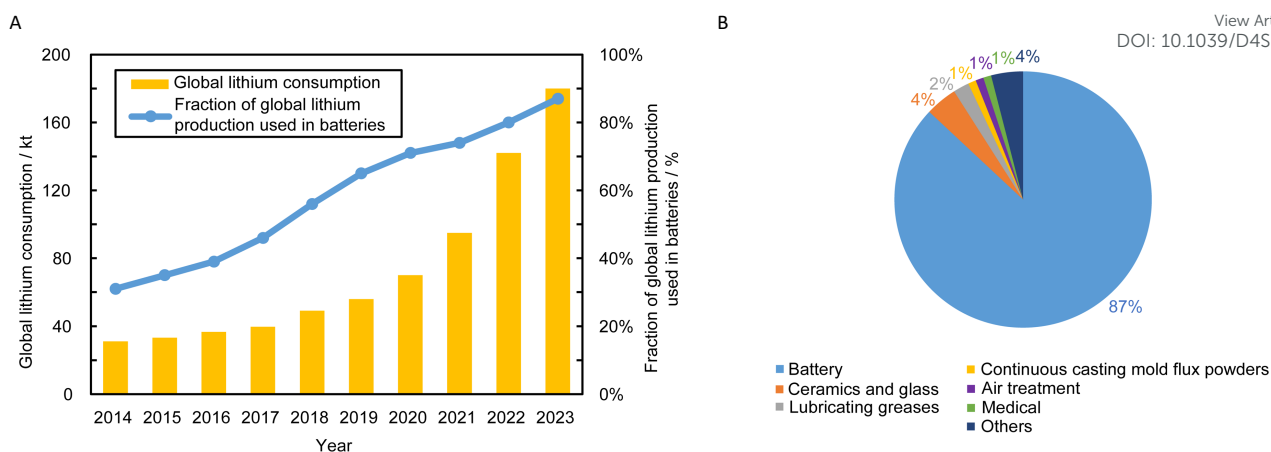
Fig. 1. (A) Global lithium consumption and proportion of battery field in a decade. (B) Lithium consumption in different industries in 2023.[1]

Amongst industrial effluents, the formation water produced during oil and gas extraction activities can be considered a potential lithium(I) source, although such brines are typically regarded as waste and are reinjected into the subsurface for disposal.[10] In these brines, lithium concentrations generally range between 1 and 40 mg dm^{-3} and depend on the geology of the field.[11] While lithium(I) concentrations in seawater are typically 0.1 -0.2 mg dm^{-3}, as mentioned above, brines from reverse osmosis processes used to desalinate seawater contain Li^{I} concentrations up to 4 mg dm^{-3}, so are more promising potential Li^{I} sources compared to seawater.[12] Industrial wastewaters, e.g. from cobalt or nickel recovery processes of lithium-ion battery recycling, can contain up to 3 g Li^{I} dm^{-3}.[13–15] Recovery of lithium(I) from such resources could enable the industry to develop a circular economy and a strategy to enhance the sustainability of the lithium(I) value chain. Nevertheless, high specific energy consumptions, high costs, Li^{I} selectivities against other cations present and slow process kinetics remain significant challenges, requiring further R&D to increase and optimise Li^{I} recoveries from industrial effluents.

Lithium(I) concentrations in the South American Atacama desert brines reach 1,500 ppm.[16] Salt lake brines are thought to contain over 70 % of exploitable lithium(I) resources globally,[1] and about 85 % of lithium(I) products are obtained from brines.[17,18] However, salt lake brines have extremely complex compositions, with Na$^+$ constituting the greatest proportion of cations, including K$^+$, Mg^{2+} and Ca^{2+}, with Cl$^-$, CO$_3^{2-}$, SO$_4^{2-}$ and borate anions.[19] This causes a significant challenge for purification and selective lithium(I) extraction by various processes being developed, in addition to evaporation technology, as described in the following section. Adsorption by ion exchange of Li$^+$ ions from brine on e.g. manganese oxides, titanium dioxide, or alumina, can achieve selective recovery when saturated adsorbents in columns are washed with fresh water or acidic solution, producing lithium(I)-containing solutions. After a specific Li^{I} concentration is achieved, sodium carbonate is added to precipitate Li$_2$CO$_3$.[17,20] Alternatively, liquid-liquid extraction by various organic solvents can be used to extract LiCl selectively.[20,21] Such solvents include β-diketones, n-butanol, neutral organophosphorus compounds, and

kerosene.[21,22] Although these solvents can differentiate effectively LiCl from NaCl and KCl, separating LiCl from MgCl$_2$ is more difficult. Increasing selectivity between Li$^+$ and Mg^{2+} often necessitates significant adjustments to pH or brine composition, requiring large amounts of chemicals. Solar evaporative processes predominate in Chile, because of their low costs and as the sensitivity of the environment in the Chilean Atacama region, where water is extremely scarce, precludes processes that require large freshwater inputs to resolve pollution issues.

Common forms of lithium salts include lithium chloride (LiCl), lithium hydroxide (LiOH), and lithium carbonate (Li$_2$CO$_3$). LiCl can be sourced from lithium-rich hard rock resources, salt lake brines, geothermal brines, and from lithium battery recycling. Although LiCl is not directly usable in LIBs, it is a valuable intermediate for converting to LiOH or Li$_2$CO$_3$; the latter, a primary compound for LIB production, can be produced by reacting LiCl with Na$_2$CO$_3$,[23]. LiOH, another important compound for LIBs, can be synthesised from Li$_2$CO$_3$,[24] with research ongoing to convert LiCl directly to LiOH.[25]

The rising demand of LIBs has triggered a growing interest and a focus in quantifying the environmental burdens with the raw material production throughout its life cycle. Ellingsen (2014)[26] established a transparent LIBs LCI on primary data. With regard to lithium production in that research, it is a generalised black box model. Kallitsis (2020)[27] studied the LCA of LIBs production in China. This model was based on the model of Ellingsen (2014)[26] and is also a black box model for lithium production. However, the actual environmental impacts of lithium production are expected to be influenced by the specifics of the region and particularly the specific lithium raw material. For example, given the energy intensity of the processes involved, the environmental impact of producing Li$_2$CO$_3$ or LiOH from spodumene should have a significantly greater environmental impact than if it were from brine. Although previous research[28] suggested that the environmental impacts of Li$_2$CO$_3$ production was negligible compared to the total transportation impacts caused by an EV, possibly in another continent, they are certainly not negligible for the location where raw material production occurs. Moreover, the rapidly growing demand for lithium(I) raw material over the last decade warrants prudence. This work presents a detailed unit

process level model that has been developed as a necessary tool to establish a more reliable and accurate environmental impact assessment of lithium(I) production processes.

Stamp (2012)[28] established a detailed LCI model for Li_2CO_3 production by allocating the inputs of Li_2CO_3 production according to economics, which increased the accuracy of LCA analysis. However, the primary data referred within the research appears to be outdated, and the water balance was neglected. The reliance on assumptions of evaporation may contribute to an inaccurate evaporation efficiency. Kelly (2021)[29] reported a detailed LCI of Li_2CO_3 production from brine, but the electrical energy used for analysis is the average Chilean electrical grid fuel mix, overlooking the fact that the national Chilean electrical grid contains different regional grids with distinct fuel mixes. The composition of the regional electrical grid varies according to different climatic characteristics across the nation. For instance, the northern region has abundant solar and wind energy resources. However, coal-fired power plants are also predominantly located in the central and northern regions of Chile.[30] Chordia (2022)[31] updated the life cycle environmental impacts of lithium from brine. Their LCI covered several literatures, technical reports, and Ecoinvent database, but it only offers inputs and outputs without explaining sufficiently the calculation procedures used, nor do they account for the electrical grid mix. Furthermore, the freshwater resources are considered to be extracted from underground aquifers instead of lake-sourced fresh water which is reported in the literature. In contrast, this research reported here accounts for the separation of minerals from brines and allows for a better understanding of water footprint throughout the process. Khakmardan et al. (2023)[32] reported LCA results of different lithium(I) production processes from a global perspective and compared the environmental impacts of lithium production processes from different sources, including brine (Chile), spodumene (Australia and China), hectorite (Mexico), and zinnwaldite (Germany). Lithium(I) production from Chilean brine had the lowest GWP and minimal water consumption, due primarily to the less energy-intensive nature of the brine production process, which involves only pumping the brine to solar evaporation ponds and concentrating it progressively by solar radiation. In contrast, the production of lithium(I) from hard rock sources requires energy-intensive processes such as crushing, grinding, desliming, and flotation, as well as leaching processes and the use of soda ash, sodium hydroxide, and sulfuric acids, which significantly increase water consumption. However, the detailed LCI data of this study is not available for verification. Moreover, the lack of high-quality publicly available data has led to high uncertainty in the results reported.

WF and WSF are increasingly important considerations in the LCA analysis, especially when considering operations taking place in extremely arid regions. Despite the general awareness around this topic, there is still a conceptual debate as to whether including brine water in water footprint analysis in appropriate. Some literature only considers freshwater consumption and excludes brine water from the scope of water consumption due to the unsuitability of brines for direct agricultural or domestic use,[29,31–33] while other literature considers it as the extraction of brine is not accounted for in the depletion of abiotic resources, where extraction of rock minerals extraction impacts are accounted for.[34] In addition, the water scarcity characterisation factors of different regions can also influence the results. In arid regions, the regional water scarcity characterisation factors will be higher than those of other non-arid regions, thereby reflecting in the overall water scarcity impact.[35] Therefore, it is crucial to specify details and relevant parameters in both WF and WSF analysis.

This study addresses the environmental impacts and water consumption of producing battery-grade Li_2CO_3 from lithium-containing brine. For this, a detailed LCI modelling of the processes used to extract lithium from resources at Salar de Atacama, Chile, was conducted based on state-of-art literature, technical reports, and Ecoinvent database version 3.9.1.[36] The electrical grid mix of the northern Chile region was modelled. Aspen Plus V11[37] is utilised to simulate the production process of Li_2CO_3, including the recycling of input materials. Furthermore, evaporation modelling and water balance were conducted, followed by WF and WSF analysis. The LCA modelling was conducted within the Sphera software.[38] Based on the ReCiPe 2016 v1.1 Midpoint characterisation method, 13 relevant environmental impacts were analysed and their primary contributions are discussed.

2. Methods

2.1 Life Cycle Assessment methodology

Following the ISO standard,[39] a detailed LCI analysis and life cycle assessments were developed to analyse the production of Li_2CO_3.

2.1.1. Goal and Scope The functional unit was set as the production of 1 kg of Li_2CO_3 of 99.5 % purity. The geographical boundary was restricted to Chile, including material inputs, manufacturing processes, transportation, electrical grid mix and other relevant factors. The system boundary was from cradle-to-gate, which includes mining and pumping of brine, evaporation processes, transportation, and chemical manufacturing in a local plant.

2.1.2 Life Cycle Inventory Analysis The LCI of Li_2CO_3 production from brine was modelled, having identified the detailed chemical production process, with specific environment and technical parameters from the literature, technical reports and the Ecoinvent database 3.9.1.[33,40,41]

Calculations for material inputs and outputs were based on stoichiometries with the necessary adjustments required to account for the incompleteness of chemical reactions. Subsequently, the production process was simulated using Aspen Plus V11.[37] In addition, the economic allocation approach was applied to Li_2CO_3 production of material and energy inputs according to ISO 14040,[39] as there are by-products such as potassium sulphate which are also produced during evaporation with their market prices collected from up to date company reports which are used as economic allocation factors.

ARTICLE

Journal Name

[41] Infrastructure construction is not considered in this study due to data unavailability, also considering that this is amortised over the economic materials production during the whole life of the facilities.

The process routes of Li_2CO_3 production from Atacama brine are given in Fig. 2. Firstly, underground brine is pumped from the subsurface at the Salar de Atacama core region and deposited into a series of large open-air evaporation ponds to evaporate by solar energy to preconcentrate lithium. The common order of precipitation includes halite (NaCl), sylvite (KCl), sylvinite (KCl and NaCl), magnesium salts and small quantities of other alkali salts.[42] In order to account for the evaporation process impacts, simulation and calculations using estimation, theoretical calculations based on the Penman equation,[43] and reported measurement data from an on-site meteorological station[44] have been used. Detailed explanations of evaporation modelling are provided in subsequent sections. In the Atacama Desert region, freshwater is reported to be extracted from 4 groundwater wells from beneath the foothills of the eastern mountains of the desert.[41] After lithium chloride has reached the drying-up point, at a concentration of approximately 6,000 ppm,[17] the concentrated brine is trucked 230 km from desert core to a chemical plant, and is then processed to remove impurities. Treatments include acidification, solvent extraction, re-extraction, precipitation and drying. Borates are removed by acidification and solvent extraction. Re-extraction is used for recycling the organic solvent. Mg^{II} and Ca^{II} are removed by precipitation with soda ash and lime milk. Solid and liquid wastes are collected in surface impoundment. The final concentrated brine is carbonised with soda ash, thereby precipitating the Li_2CO_3 product. After washing, drying, and packaging, Li_2CO_3 product can be obtained. Water is used primarily for cleaning pipes at the salar evaporation ponds and as wash water in the production process at the plant. Additionally, water is used for preparing solutions, e.g. of Na_2CO_3. Electrical energy is used mainly for operating machinery and equipment such as pumps,

filters, reactors, dryers, as well as for powering various facilities within the production process. The production process primarily relies on energy supplied by the electrical grid and fossil fuels. For the electrical grid mix, the SING (Sistema Interconectado del Norte Grande) electrical grid in northern Chile region is chosen for modelling.[30,45]

The process modelling was carried out for Li_2CO_3 production in the chemical plant using Aspen Plus V11.[37] A heat exchange network was constructed together with the process. The modelling method was set as ELECNRTL. The life cycle inventory is optimised by iteration with Aspen modelling results.

2.1.3 Life Cycle Impact Assessment In order to evaluate the environmental impact of LI_2CO_3 product from brine, LCA modelling was conducted using Sphera software.[38] The background processes were retrieved from the Ecoinvent database 3.9.1.[36] The ReCiPe 2016 v1.1 Midpoint characterisation method and the partly regionalised WSF based on AWARE method[35] were used for analysis.

2.2 Weather Condition and Evaporation Modelling

2.2.1 Weather condition at Salar de Atacama Lithium production from brine is mainly determined by its composition, volume, accessibility, and suitability for local processing.[9] In the Atacama Desert, the climatic conditions are suitable for implementation of a relatively simple evaporation technology. The weather data used here were collected from meteorological stations operated by SQM at the Atacama Desert core,[44] together with regional data from the meteorological directorate of Chile.[46] The monthly precipitation rate and temperature at the Atacama Desert is shown in Fig. 3.

The weather in the Atacama Desert is extremely arid. The average annual precipitation is around 20 mm a^{-1}, and the annual precipitation rate of the core region is less than 10 mm a^{-1}.[44] The precipitation has seasonal variations, the summer months from February to April have a relatively high level of precipitation which reached 2.1 mm in 2023, while there is no
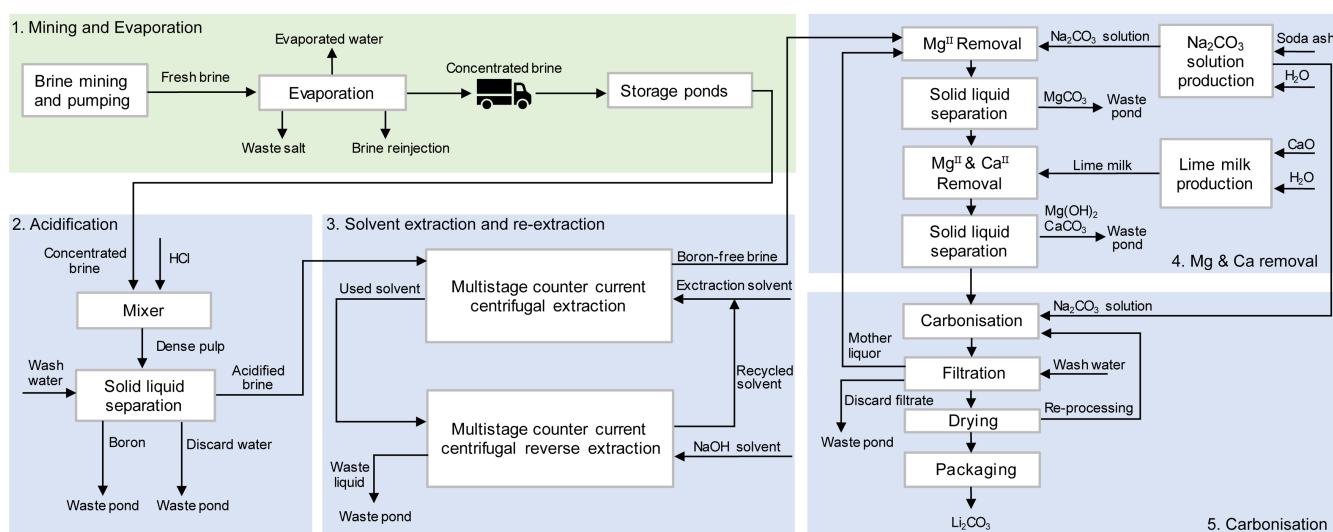

Fig. 2. Lithium carbonate production process flow.

precipitation during May to December. The total annual precipitation rate at the Atacama core region is 7.4 mm a⁻¹. As shown in Fig. 3, the average daily temperatures typically peak at approximately 18.9 °C and reach a minimum of around 8.32 °C in June. Diurnal temperature fluctuations match this seasonal variability, with maximum and minimum daily temperatures typically separated by around 14 °C.[46] During October to March, winds blow predominantly from the west, and during autumn and winter, the wind direction is more variable. Morning wind speeds throughout the year are generally < 2 m s⁻¹, and wind speeds typically increase in the afternoon, reaching up to 15 m s⁻¹.[47] The low precipitation and high solar insolation make this place favourable for evaporation technology. Overall, producing lithium from brine at arid region is cost-effective.
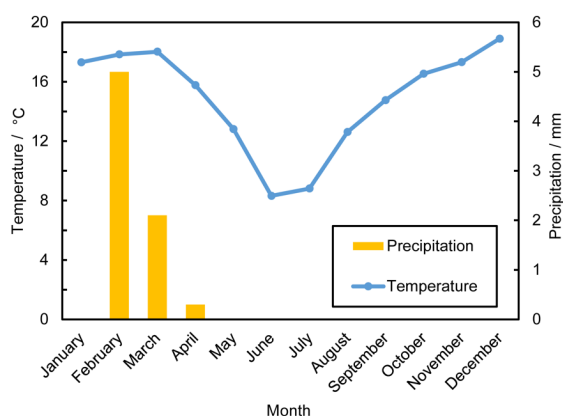

Fig. 3. Monthly precipitation rate and temperature at Atacama Desert in 2023.[44,46]

Although this is an inexpensive technology as naturally solar energy is easily available in the Atacama Desert region, there are still some disadvantages. The evaporation precipitation steps are time-consuming, which normally takes up between 8-12 months,[41] and may take longer time, up to even 24 months from the pumping process.[17,48] Besides, the significant amount of water evaporation from brine, which cannot be recovered, may cause a series of hydrological and environmental issues.

2.2.2 Evaporation modelling Three methods are used to simulate the evaporation process. Firstly, it is assumed that up to 95 % of brine water need to be evaporated.[49] In the second approach, the evaporation rate is calculated using the simplified Penman equation.[43] Thirdly, evaporation data measured by Class A pan of the on-site meteorological station near the evaporation ponds[44] is used. It is important to note that the evaporation rate of brine can be influenced by weather and salinity during evaporation, which can severely reduce the evaporation rate, so a correction is necessary.[50–53]

The theoretical method based on the simplified version of Penman's equations is as follows: [43]

$$E_{\text{PEN}} \approx 0.051(1 - \alpha)R_S\sqrt{T + 9.5} - 2.4\left(\frac{R_S}{R_A}\right)^2$$

$$+0.052(T + 20)\left(1 - \frac{RH}{100}\right)(a_U - 0.38 + 0.54u) \tag{1}$$

Where

$$R_S = R_A\left(0.5 + 0.25\frac{n}{N}\right) \tag{2}$$

$$N \approx 4\emptyset sin(0.53i - 1.65) + 12 \tag{3}$$

$$R_A \approx 3Nsin(0.131N - 0.95\emptyset) \text{ for } |\emptyset| > \frac{23.5\pi}{180} \tag{4}$$

E_{PEN} represents the evaporation rate in mm day⁻¹ calculated by the Penman equation; α the albedo, 0.08 for open water surfaces; R_S the solar irradiance in MJ m⁻² day⁻¹. It can be calculated, if R_A, the extraterrestrial irradiance (MJ m⁻² day⁻¹), n, the bright sunshine hours per day (h), and N, the maximum possible duration of daylight (h) are known. T is the average temperature (°C); RH is the relative humidity (%); a_U equals 1 when original N can be calculated if $\emptyset$, the latitude of the site in radians, which is negative for south, and i, the rank of month is known. For temperate zone where $|\emptyset| > \frac{23.5\pi}{180}$, R_A can be calculated if direct data is not available.

The correction equation for the evaporation rate is as follows:[54]

$$E_O = K_e K_S E_t \tag{5}$$

E_O corresponds to the corrected evaporation rate in mm day⁻¹; E_t is the recorded of evaporation in the class A pan or calculations in mm day⁻¹; K_e is a dimensionless correction factor, the pond coefficient which equals 0.7. This coefficient is related to weather and was estimated in the United States, which has similar weather conditions to those that occur at the Atacama Desert region. K_S is the salinity reduction coefficient, which also is a dimensionless correction factor and related to liquid average density, which can be determined by the method outlined in IDE (1978).[55]

2.3 Water Balance

2.3.1 Water balance Water resources issues regarding evaporation processes in the Atacama Desert have still been an open question. Both brine and fresh water are utilised during the brine extraction processes. Up to 95% of the water content in the brine is lost during evaporation, resulting in a concentrated lithium brine. Whether the brine is considered a water resource is still a controversial issue, which brings questions to water balance research.

Brines, which are neither suitable for human use, nor for irrigation, are designated as minerals rather than water resources.[56] However, plants and animals that inhabit the Atacama region depend on this water resource, including protected species such as flamingos. Changes in flamingo populations can strongly reflect the extent of environmental damage. Andean and James' flamingos, which are the most threatened species in the Salar de Atacama, declined by approximately 12% and 10% in recent years.[57] Studies have shown a strong correlation between lithium mining activities and local environmental degradation in Atacama.[57,58] However, the direct impact of lithium extraction on the environment and

hydrology of the Atacama region has not been stated with certainty.

In this research, minerals and water in the brine are suggested to be considered separately to investigate the water balance of the system. Water contained in the brine is considered as water resource for water balance calculations.[33] Calculating the water balance provides a clearer understanding of the amount of water that needs to be added and the amount of water flowing out of the system. Eq. (6) shows the mass balance of the inputs and outputs in a unit process.[59]

$$W_{ei} + W_{ii} + S_i = W_o + S_o + W_w + W_r \qquad (6)$$

Where, W_{ei} represents the external water input; W_{ii} the internal water input; S_i the solid input; W_o the water output; S_o the solid output; W_w the wastewater and W_r the recycled water, as shown in Fig. 4.
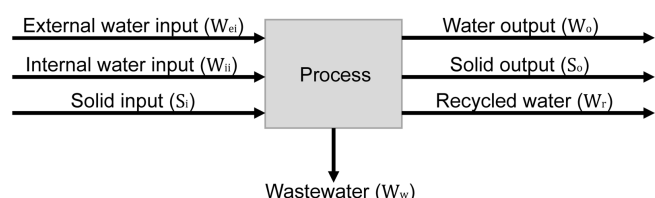

Fig. 4. Water mass balance in an individual unit process.

2.3.2 Water footprint and water scarcity The WF is divided into three categories:[60] the blue WF which is the consumption of surface and ground water; the green WF is the consumption of precipitation; the grey WF is the consumption of freshwater used to dilute pollutants. Although precipitation is very low, green water and blue water were considered in this study. The blue water includes the water incorporated in final product, evaporation, and discharge of used water. Besides, the consumption includes direct consumption and embodied water consumption, which is the WF of materials used in process. Water consumption in Li_2CO_3 plant is estimated based on water balance studies. In addition, the WSF can be analysed and provide a more comprehensive understanding and comparable results of the impact of the production on water resources in a specific region. The water scarcity characterisation factor is determined here using the AWARE method, defined for Chile as 81.38 m³ world equivalent per m³.[35]

2.4 Waste Management

During the evaporation production process, a significant amount of salt waste and used brine are generated. The salt waste is typically accumulated near the evaporation ponds on open ground,[41] while used brine is reinjected into the subsurface.[61] However, to the best of our knowledge, there is no reported precise operational details or real case studies of reinjection of large volume of spent brine. The question whether reinjecting brine may cause dilution of lithium resources, change the ecosystem, or disrupt the stratigraphic

structure in Atacama still remains a controversial and unresolved issue.[17] Considering the aforementioned conditions, detailed reinjection analysis is not within the scope of this research. Similarly, during the Li_2CO_3 production in the chemical plant, the process generates solid and liquid waste. The composition of liquid waste comprises water with boron, organics and some mother liquor containing impurities; while the solid wastes are magnesium carbonate pulp, magnesium hydroxide pulp and calcium carbonate pulp which is generated from precipitation processes. The industrial wastes are disposed in impoundments.[41]

Traditional LCA studies typically neglect the influence of waste management units. However, studying the impact of waste management units is necessary in an arid location like the Atacama Desert where rare animals are present. This study aimed to investigate whether current waste management methods have an impact on the infiltration of groundwater and brine and assess the rational of current waste management practices. The waste management units considered include waste salt piles and surface impoundments.

2.7.1 Life Cycle Model for Waste salt piles Waste piles are facilities where waste is placed for disposal as shown in Fig. 5. However, the leachate from landfills may have negative effects on the groundwater in the surrounding area.
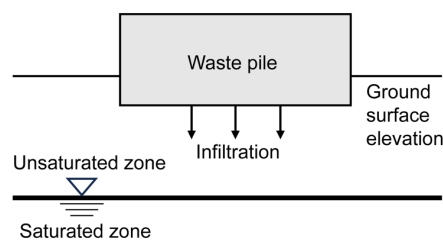

Fig. 5. Waste pile structure illustration.

The waste pile is modelled here as a rectangular prism model with rainfall as input and leachate as output. The precipitation can be stored in the system, drained laterally, or evaporated back into the atmosphere, as there is little plant cover in the Atacama production region, the plant evapotranspiration is not considered. As the precipitation and temperature fluctuate with seasons, the quantity of water that is infiltrating is calculated using the principle of annual water balance, as following Eq. (7):

$$I_a = P_a - E_a - (FC - W) \times T_a \qquad (7)$$

Where, I_a is the annual water infiltration (mm year⁻¹); P_a is the annual precipitation in (mm year⁻¹); E_a is the annual evaporation (mm year⁻¹); FC is the field capacity (vol vol⁻¹); W is the initial water content of the fresh waste (vol vol⁻¹); T_a is the thickness of the fresh waste layer accumulated (mm year⁻¹).

2.7.2 Life Cycle Model for Surface Impoundments There are three options of configuration of surface impoundment considered here: unlined, single liner and composite liner as shown in Fig. 6. The equations and illustrations of the average infiltration rate of the unlined and single lined scenarios are

respectively shown in Eq. (8) and (9), while for the case of composite liner, the leakage rate is calculated in Eq. (10).[62]

$$I = \frac{H_p + D_{fc} + D_{clog}}{\frac{D_{fc}}{K_{fc}} + \frac{D_{clog}}{K_{clog}}} \quad (8)$$

$$I = \frac{H_p + D_{fc} + D_{liner}}{\frac{D_{fc}}{K_{fc}} + \frac{D_{liner}}{K_{liner}}} \quad (9)$$

$$Q = 0.21a^{0.1}h^{0.9}K_s^{0.74}\rho S \quad (10)$$

Where I is the average infiltration rate (m s⁻¹); H_p is the pond depth of wastewater in the surface impoundment (m); D_{fc} is the thickness of consolidated sediment layer (m); D_{clog} and D_{liner} are the thickness of clogged soil layer and consolidated sediment layer in m respectively, which is typically
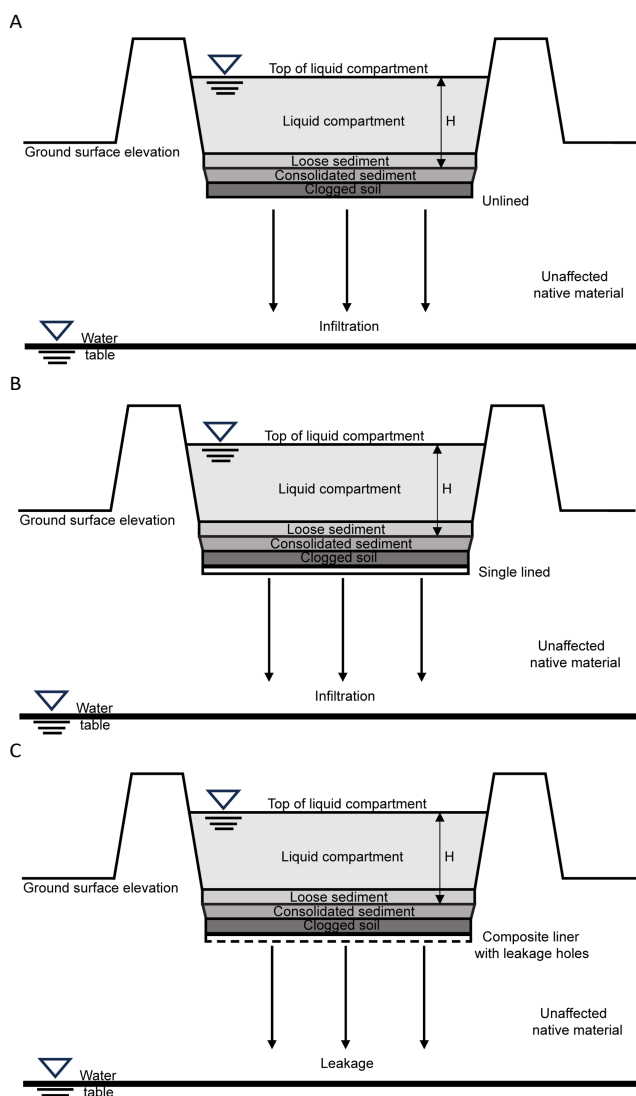
Fig. 6. Three types of surface impoundments considered. A. Unlined. B. Single lined. C. Composite liner with leakage holes.[62]

0.5 m; K_{fc} is the saturated hydraulic conductivity of consolidated sediment (m s⁻¹); K_{clog} and K_{liner} are the saturated hydraulic conductivity of clogged soil and liner respectively (m s⁻¹). For the equation of composite liner, Q is the steady-state rate of leakage through holes in the composite liner (m³ s⁻¹); a is the area of holes in the geomembrane (m²); h is the head of liquid on top of geomembrane (m); K_S is the hydraulic conductivity of the low-permeability soil underlying the geomembrane (m s⁻¹); ρ is the leak density (holes m⁻²); S is the footprint of the surface impoundment (m²). The required parameters can be obtained from USEPA (2003a).[63]

3. Results and Discussion

3.1 Life Cycle Inventory (LCI) Analysis

The following sections provide a detailed analysis of the LCI results for Li₂CO₃ production from the Atacama Desert brines. The results presented and discussed start from the process modelling.

3.1.1. Process modelling. The Li₂CO₃ production simulation results provide quantified inputs and outputs at unit process level. After solar evaporation, the concentrated brine is transferred to the chemical plant in which it is acidified with hydrochloric acid, followed by filtration to remove insoluble borates formed with divalent cations (e.g. CaB₄O₇.6H₂0), then soluble boron(III) species are extracted by organic solvents in a multistage counter-current centrifugal extraction process. The boron(III) species in the reacted organic solvent is then re-extracted into aqueous NaOH, requiring 6.72 kg NaOH per kg of Li₂CO₃ product. The then boron(III)-free brine is reacted with Na₂CO₃ to precipitate and recover part of the Mg^{II} as MgCO₃, followed by Mg^{II} and Ca^{II} removal as carbonates using lime water, which is cheaper than a Na₂CO₃ solution. Finally, the purified brine is reacted with Na₂CO₃ to precipitate Li₂CO₃, recovered by filtration, then washed with cold water and dried at 150 °C for 3 hours to obtain the final battery-grade product. The mother liquor generated during the carbonisation process can be used to dilute boron-free brine, thereby decreasing the loss of lithium(I) during Mg^{II} and Ca^{II} precipitation.

The simulation results showed that for the chemical plant to produce 1 kg of Li₂CO₃, it required 3.28 kg concentrated brine, and 0.13 kg, 2.79 kg and 10.71 kg of hydrochloric acid, organic solvent, and hydrocarbon diluent, respectively. Precipitation of Mg^{II} and Ca^{II} impurities and carbonisation of the lithium(I) product required 5.79 kg Na₂CO₃ in aqueous solution, together with 0.014 kg of lime water. The Aspen modelling of the Li₂CO₃ production process validated the LCI inputs and outputs; finally, discrepancies between modelled results and calculated and the collected LCI data inputs were optimised by modelling.

3.1.2. Evaporation modelling. Previous publications on LCI on the Li₂CO₃ production process appear to have overlooked evaporation rate modelling, which was investigated here by correction and comparison of assumptions, theoretical calculations and measured results. The assumption generally made by previous researchers,[17,49] that up to 95 % of the brine is evaporated, resulted in a corrected brine evaporation rate of 2.71 mm day⁻¹. The Chilean company Sociedad Química y

ARTICLE

Minera (SQM) has reported measured brine evaporation rates of 3.24 mm day^{-1}, using a metal Class A evaporation pan at its measurement stations on site in the Atacama region. The corrected evaporation rate of brine calculated using Penman's Eq. (1) was 2.62 mm day^{-1}. The estimated result based on earlier authors is similar to that, but significantly lower than that measured by the Class A pan, possibly because the side of the pan was also exposed to sunlight, potentially leading to an overestimation of the evaporation rate.[64] Additionally, the liquid placed in the pan for testing is not sufficiently specified, thus it is uncertain whether it is brine, groundwater, or some other water. For the theoretical calculation, a simplified version of Penman's equation was used, acknowledging that the wind speed may have a significant effect on the evaporation rate. The evaporation modelling results were used to devise three scenarios in the water balance analysis, as explained in section 3.2.2.

3.1.3. Electrical grid fuel mix. As shown in Fig. 7, the main fuels of the SING electrical grid mix in 2023 were 48.46 % natural gas and 34.80 % hard coal, accounting for 83.26% of the total electrical grid mix, to which 8.7 % was added from photovoltaic energy, due to the abundant solar energy resources in the northern Chile region. Hydropower, diesel, fuel geothermal and cogeneration contributed less to the SING electrical grid mix. Although this specification is very carbon intensive, it is expected that the percentage of coal based power will decrease with time due to the stated intentions in Chilean government's energy policy, aiming to decommission coal-fired power plants and increase the utilisation of solar power.[30]

3.1.4. Waste management. The average water infiltration can be calculated by Eq. (7) to (10). Evidently, the climate in the Atacama desert is extremely arid, as the measured annual precipitation is 7.4 mm year^{-1}, while the measured evaporation is 3,246.9 mm year^{-1}.[44] The value of T_a in Eq. (7) cannot be obtained, but the maximum height of waste piles is 30 m.[41] Although the exact values of FC and W are not available, assuming a value of 1 for FC and 0 for W, it can still be estimated that the predicted infiltration will be less than zero. This indicates that there is hardly liquid infiltration from the waste piles formed to the lower layers. Therefore, the infiltration of waste salt from piles will likely have minimal impact on groundwater quality. Similarly, for the infiltration analysis of surface impoundments, whether unlined, single lined or composite lined, the infiltration rate and leakage are extremely small. As a result of the range of values for parameters K_{fc} and a, for the unlined model, the average infiltration rate was predicted to range from 2.24×10^{-7} m s^{-1} to 3.07×10^{-7} m s^{-1}; for the single lined model, the infiltration rate ranged from 1.94×10^{-8} m s^{-1} to 1.98×10^{-8} m s^{-1}; for the composite liner model, the leakage ranged from 4.83×10^{-8} m s^{-1} to 6.09×10^{-8} m s^{-1}. Consequently, infiltration may have little influence on underground water and brine. Therefore, it is perceived that rainwater management or a collection system may not be needed.
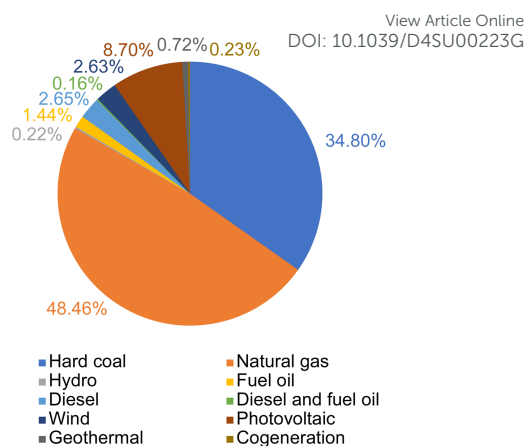
Fig. 7. Northern Chilean electrical fuel grid mix.[45]

While the impact of waste infiltration may be negligible, the waste produced during evaporation and accumulated near the evaporation ponds occupies significant land area. Based on calculations, the annual production of 1.8×10^5 tonnes a^{-1} of Li$_2$CO$_3$ will generate 1.43×10^{10} kg a^{-1} of waste salts, consisting mainly of sodium and potassium salts. As assumed by Flexer (2018),[17] the salt mixture was considered to have an average volumetric density of 2 kg dm^{-3}. As a result, this will produce waste with a volume of 7.16×10^6 m^3 a^{-1}. Assuming that each waste pile has a height of 30 m,[41] the total required area is 2.39×10^5 m^2 a^{-1} which is expected to expand with increasing annual production and the implementation of timely waste disposal required.

3.2 Life Cycle Impact Assessment Analysis

3.2.1. Life Cycle Impact Assessment. A cradle-to-gate LCA for producing 1 kg of Li$_2$CO$_3$ from brine was conducted based on the optimised LCI produced. Fig. 8 presents the 13 different environmental impacts assigned to different key contributing processes.

Among all impact categories, use of NaOH and sodium carbonate, water supply, and electrical energy supply were the most significant contributors, with minor additional contributions from other sources. This arose mainly from the NaOH requirement in the re-extraction process of borates from organic to aqueous solvents. As chlor-alkali production is a high-energy-consuming industry, the electrical energy requirement of the chlor-alkali electrolytic process for NaOH production was the dominant contributor. Additionally, Na$_2$CO$_3$, which is used for the Mg^{II} and Ca^{II} removal and for carbonisation of the Li$_2$CO$_3$ product, leaded to environmental impacts. The entire production process requires electrical energy from the grid and water for solution preparation and as wash water, which also given rise to significant burdens.

Despite the high CO$_2$ footprint of NaOH production being including in the analysis, as shown in Table 1, the overall GWP of the Li$_2$CO$_3$ production was predicted as 5.82 kg CO$_2$ (kg Li$_2$CO$_3$)$^{-1}$, driven primarily by use of NaOH (75.84 %), Na$_2$CO$_3$ (14.01 %) and electrical energy (8.30 %). If the re-extraction
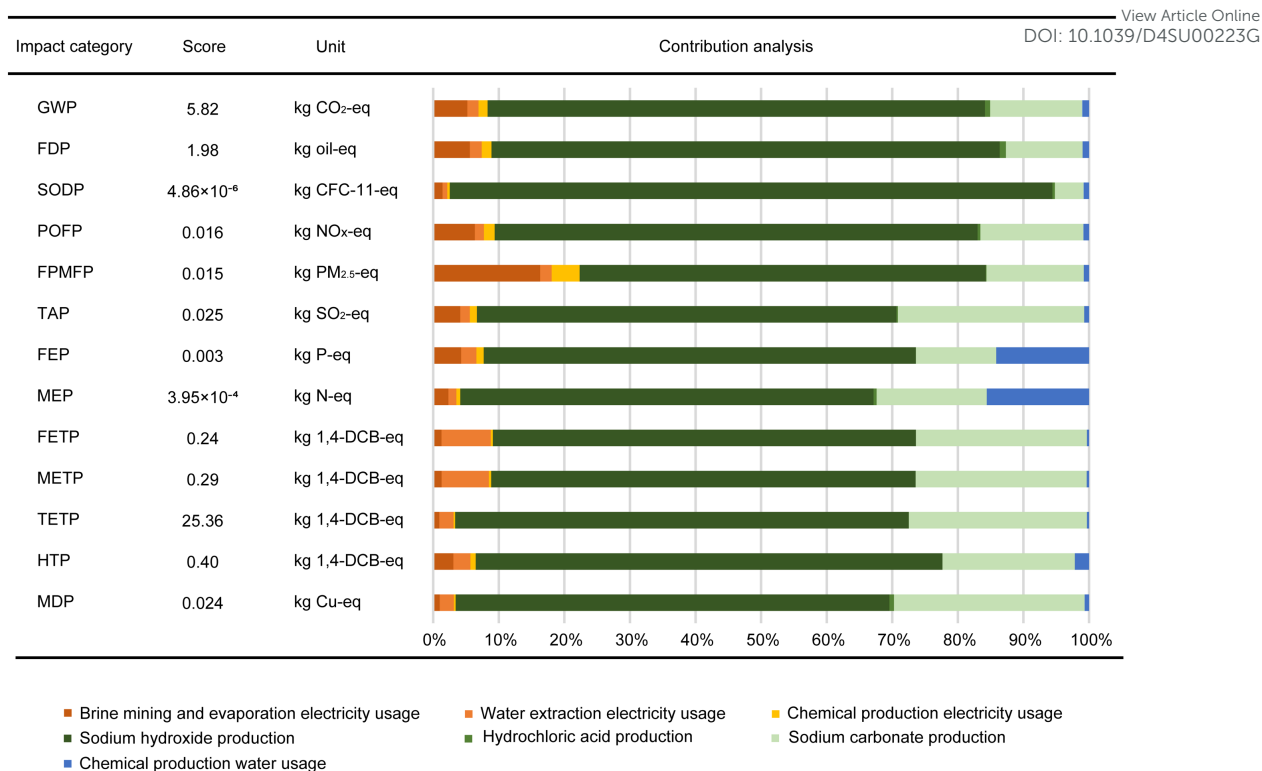
Fig. 8. Environmental impacts of lithium carbonate production at the Atacama Desert, disaggregated to key contributing processes.

Table 1. Major environmental impact contributors for Li_2CO_3 production.

Impact	Major contributions
GWP	NaOH (75.84 %), Na_2CO_3 (14.01 %), Electricity (8.30 %)
FDP	NaOH (77.56 %), Na_2CO_3 (11.67 %)
SODP	NaOH (91.89 %), Na_2CO_3 (4.37 %)
POFP	NaOH (73.64 %), Na_2CO_3 (15.71 %)
FPMFP	NaOH (61.90 %), Electricity (18.08 %), Na_2CO_3 (14.83 %)
TAP	NaOH (63.97 %), Na_2CO_3 (28.40 %)
FEP	NaOH (65.89 %), Na_2CO_3 (12.23 %), Water (14.15 %)
MEP	NaOH (63.02 %), Na_2CO_3 (16.80 %), Water (15.60 %)
FETP	NaOH (64.49 %), Na_2CO_3 (26.05 %)
METP	NaOH (64.71 %), Na_2CO_3 (26.10 %)
TETP	NaOH (69.14 %), Na_2CO_3 (27.14 %)
HTP	NaOH (71.16 %), Na_2CO_3 (20.17 %), Water (2.17 %)
MDP	NaOH (66.13 %), Na_2CO_3 (29.06 %)

process was not included in the production process, the overall GWP was predicted to decrease to 1.41 kg CO_2 (kg $Li_2CO_3)^{-1}$. However, this would result in increased costs and large volumes of waste organic solvents to be treated. The major environmental impacts contributors are summarised in Table 1. NaOH, Na_2CO_3, electrical energy and water use were the dominant contributors to fossil depletion potential (FDP), stratospheric ozone depletion (SODP), photochemical ozone formation, human health (POFP), terrestrial acidification (TAP),

freshwater ecotoxicity (FETP), marine ecotoxicity (METP), terrestrial ecotoxicity (TETP), human toxicity, cancer (HTP) and metal depletion (MDP). For fine particulate matter formation potential (FPMFP), electrical energy was the second largest contributor accounting for 18.08 %. For freshwater eutrophication (FEP) and marine eutrophication (MEP), water use contributed (14.15 % and 15.60 %, respectively), as did Na_2CO_3 (12.23 % and 16.80 %, respectively).

Table 2. GWP results comparisons of Li_2CO_3 production from brine with previous research.

Study year	GWP / kg CO_2 (kg $Li_2CO_3)^{-1}$	Reference
2012	2.02	28
2021	2.9	29
2022	3.5	31
2023	4~5	32
2024	5.82	This study

Fig. 8 reports a predicted GWP of 5.82 kg CO_2 (kg $Li_2CO_3)^{-1}$ produced from brine, whereas previously research reported different GWP values shown in Table 2.[28,29,31,32] However, it is important to note that previous results were predicted using simplistic unit process approaches without detailed theoretical calculations and modelling, such as of evaporation. It is unclear whether those authors considered the effects of boron(III) re-extraction processes, they did not include effects of regional electrical energy simulations, and used data across different years, so a range of GWP values are justified.
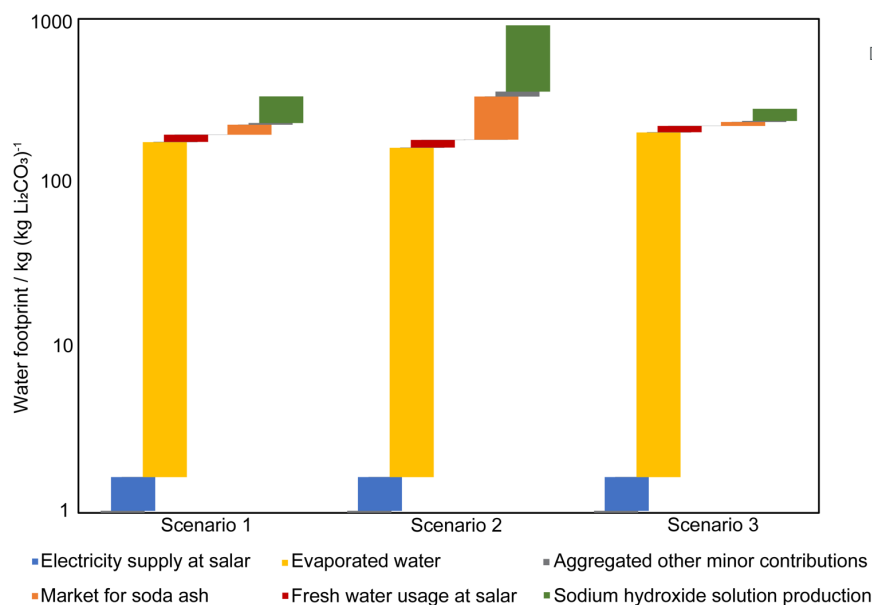
RSC Sustainability

ARTICLE

Journal Name

Fig. 9. Water footprint components for lithium carbonate production in the Atacama Desert.

3.2.2. Water footprint (WF) and water scarcity footprint (WSF). Water balance analyses were used to calculate water footprints and water scarcity footprints reported in Fig. 9. The blue WF was predicted for three different evaporation modelling scenarios, with a production period of one year; the green WF was negligible due to the limited precipitation. The minor contributors to water footprint were aggregated and detailed information can be found in the supporting information.

For the assumed evaporation scenario 1, the total blue WF was 160 kg per kg Li_2CO_3 without considering water evaporation from brine, and the chemical plant production process blue WF accounted for 87.50 % of the total. The NaOH production process consumed a significant amount of water, accounting for 74.83 % of the total blue WF of the chemical plant production process. Excluding the NaOH production process, the total blue WF for all other processes was 55.41 kg per kg Li_2CO_3. If water evaporation from brine was considered as a consumption of underground water resources, the blue WF would increase by 175.8 kg per kg Li_2CO_3.

For scenario 2, using Penman's equation (1), the total blue WF was predicted as 749 kg (kg $Li_2CO_3)^{-1}$ without considering water evaporation from brine, since decreased evaporation rates led to increased volumes of concentrated brine supplied to the chemical plant. According to the calculations, the quantity of chemicals added was proportional to the brine volume, which increased the overall water footprint. Therefore, the first process of brine evaporation is crucial as it influences the inputs to the chemical plant and water consumption, thereby affecting production processes and costs. Similarly, if water evaporation from brine was considered, the blue WF would increase by 164 kg per kg Li_2CO_3.

For scenario 3, the measured evaporation rate scenario, according to calculations, the blue WF consumption was 80 kg per kg Li_2CO_3 without considering water evaporation from brine, with 75.14 % attributed to the chemical plant production and

24.86% to the mining and evaporation processes. The actual amount of brine available for evaporation, calculated from the total annual brine extraction was 179.7 kg per kg Li_2CO_3. However, due to the higher evaporation rate, there was an excessive water evaporation from brine; the amount of evaporated water should be 202.6 kg per kg Li_2CO_3, which is 12.73 % more than the actual value.

Fig. 10 shows the WSF for Li_2CO_3 production from brine in Chile. The 2023 AWARE water scarcity index for Chile is 81.38 $m^3_{world\ eq}$ (kg $Li_2CO_3)^{-1}$.[35] The WSFs were calculated taking water evaporation from brine into account for the three scenarios: 27.45 $m^3_{world\ eq}$ (kg $Li_2CO_3)^{-1}$ for scenario 1, 74.55 $m^3_{world\ eq}$ (kg $Li_2CO_3)^{-1}$ for scenario 2 and 23.12 $m^3_{world\ eq}$ (kg $Li_2CO_3)^{-1}$ for scenario 3. The water scarcity effects of the Atacama Desert arise primarily from water evaporation from brine and direct utilisation of freshwater at the processing plant. If the prior brine evaporation concentration process is sufficient, the water demand for the processing plant would be relatively reasonable.
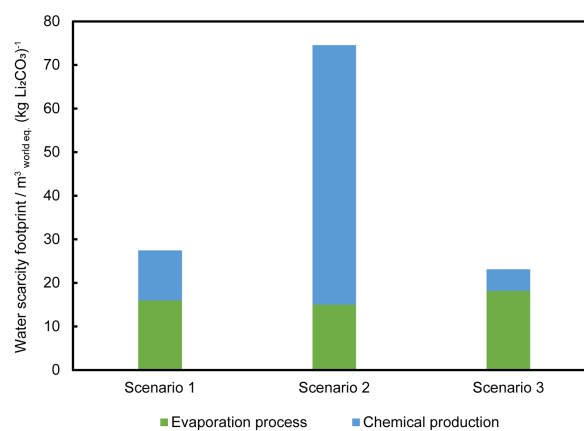

Fig. 10. Water scarcity footprint results for three scenarios: Scenario 1 for an assumed evaporation rate; Scenario 2 for Penman's equation; Scenario 3 using measured evaporation rates with the class A pan.

Some reports argue that the impact of brine extraction should not be included in water balance analyses, but should be evaluated through the hydrogeology analysis of the salt flats.[58,65,66] However, the extracted brine, through the evaporation process, results in concentrated brine and takes part in the overall water balance of the system. Therefore, we suggested that it should be considered within the complete scope of water analysis. Furthermore, the extremely high-water scarcity factor of Chile indicates the need for cautious water resource consumption in arid regions, especially in the Atacama Desert where the WSF may be even higher than the national average. It is essential to decrease water use and increase water recycling. However, presently, the evaporated brine which should be considered as a resource as well, exits the system and cannot be recovered by conventional evaporation methods. The development of new technology avoiding water evaporation from brine and reducing the amount of chemical usage will greatly benefit the arid region by reducing its water scarcity effect.

3.2.3 Sensitivity analysis. The Chilean electrical grid fuel mix and variations in brine concentration were identified as critical parameters for sensitivity analysis. These factors were analysed to evaluate their effects on the overall environmental impacts. Between 2030 and 2050, Chile's electrical grid fuel mix is set to undergo significant changes to form a more sustainable energy future, driven by a strong shift towards renewable energy sources. As shown in Table 3, the share of wind and photovoltaic energy will increase significantly. Concentrated solar power and battery energy storage will also grow.

Conversely, there will be a decrease in reliance on fossil fuels, hydropower, biomass, and geothermal energy; coal will be phased out entirely.[67]

Table 3 presents the expected Chilean electrical grid fuel mix evolution in the near- (2030) and longer-term future (2050).[67] Fig. 11 presents the respective sensitivity analysis results comparing the base case with each of these two scenarios. The transition to increasingly renewable energy-dominated grid mixes in Chile by 2030 and 2050 results in significant environmental benefits, as compared to the present base case, including decreases in GWP, FDP, POFP, FPMFP and TAP up to 16 %. However, the energy shift also introduces new challenges. SODP, FEP, MEP, FETP, METP, TETP, HTP and MDP are expected to increase by up to 30 %, due to the renewable energy infrastructure specifics, such as the need for battery energy storage systems, solar panels, and wind turbines. Due to high Li[I] concentrations in Atacama brines, specific energy consumptions of solar evaporation processes are low.[68] Therefore, switching to clean energy sources has minimal effect on decreasing GWP (1.22 % and 2.54 %).

For the sensitivity analysis of brine concentration, it was assumed that the ratios of ion concentrations in brines remained constant, while brine concentrations were diluted by 25 % and 50 %, reflecting the exploitation of lower quality resources formed by geological and hydrological processes that remained unchanged. The compositions of the diluted brines considered are presented in Table 4.

Table 3. Chile electrical grid fuel mix in 2030 and 2050.[67]

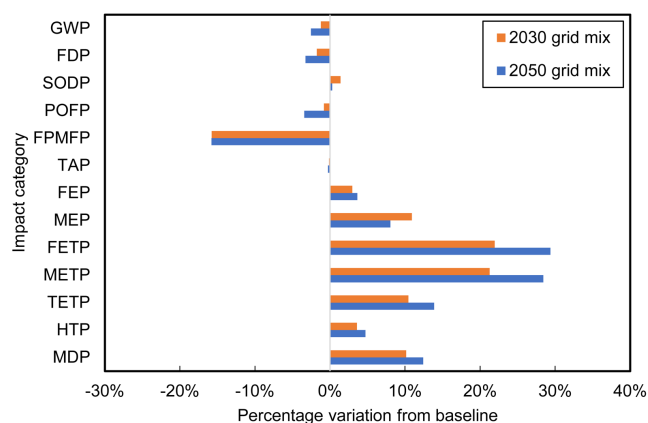| Energy type	Contribution / %	
	2030	2050
Battery energy storage system	2.32	3.17
Diesel	4.08	0.57
Wind	24.07	33.52
Photovoltaic	26.89	36.13
Concentrated solar power	13.64	17.22
Liquified natural gas	6.15	0.93
Hydro	20.09	7.30
Biomass	2.20	0.97
Geothermal	0.53	0.19
Coal	-	-

Fig. 11. Changes in life cycle impact scores of lithium carbonate production from Atacama brines due to expected electrical grid evolution.

Table 4. Brine compositions for scenarios assuming decreased concentrations of ions in brine by 25 % and 50 %.

Composition	Base case / wt.%	25 % reduction / wt.%	50 % reduction / wt.%
Li[I]	0.15	0.11	0.08
Cl[-I]	16.04	12.03	8.02
Na[I]	7.60	5.70	3.80
K[I]	1.85	1.39	0.93
Ca[II]	0.03	0.02	0.015
Mg[II]	0.96	0.72	0.48
SO$_4^{2-}$	1.65	1.24	0.83
B[III]	0.06	0.05	0.03
H$_2$O	71.66	78.75	85.83

Fig. 12 presents results of the sensitivity analysis for the two brine dilution scenarios, which were predicted to cause increases in overall environmental impacts, with life cycle impact scores increasing further as concentrations decreased. Specifically, a 25 % decrease in brine concentration led to increases in life cycle environmental impacts ranging from 33 % to 54 %, whereas a 50% reduction in brine concentration caused life cycle impacts to increase by 88 % to 126 % across the
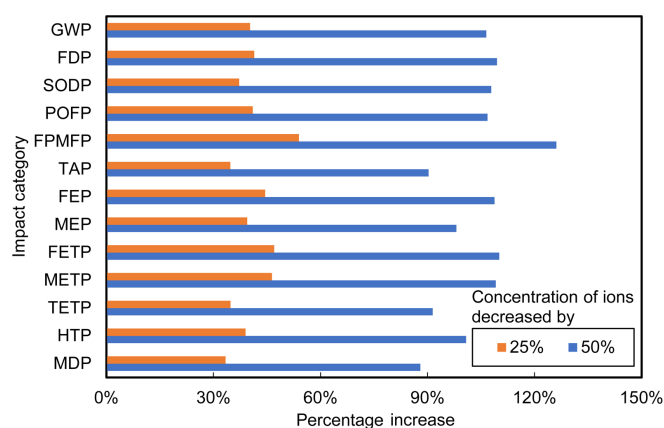
Fig. 12. Changes in life cycle impact of lithium carbonate production from Atacama brines due to 25 % and 50 % dilution of ion concentrations.

various categories. These increases were due primarily to lower brine concentrations necessitating the processing of larger volumes of brine to produce 1 kg of Li_2CO_3, in turn intensifying requirements for chemicals and energy. Consequently, overall life cycle environmental impacts increased significantly.

3.3 Process Improvements and Alternative Methods

Improvement of the present process requires optimisation of removal processes of boron(III) and other impurities. Firstly, boron(III) removal was predicted to be the primary source of pollution, mostly due to NaOH production. Replacing the hydrogen evolution / water reduction reaction ($2H_2O + 2e^- \rightarrow H_2 + 2OH^-$) at cathodes in conventional chlor-alkali membrane electrolysers with the oxygen-reduction reaction ($O_2 + 2H_2O + 4e^- \rightarrow 4OH^-$) at oxygen depolarised cathodes (ODC) could decrease of electrical energy usage by ca. 25 %, thereby decreasing CO_2 emissions and GWPs.[69] Presently, ODC technology offers the most environmentally sustainable method of chlor-alkali production.[70,71] Furthermore, molar ratios of H_2O consumed to OH^- ions produced in conventional membrane chlor-alkali processes are ca. 1, whereas that ratio is 0.5 for oxygen reduction cathodes, so enabling decreased water consumption.

Despite decades of operation of the boron(III) solvent extraction process, ongoing research is exploring alternative methods such as nanofiltration, to remove boron(III) from brine. However, nanofiltration is 1.4 to 1.7 times more polluting than solvent extraction because of its greater consumption of electrical energy.[72] In addition, the use of environmentally benign solvents and improved extraction and re-extraction techniques has the potential to decrease the consumption of input materials so decreasing environmental burdens.

Secondly, companies and academics are researching new technologies intensively to recover lithium(I) from brines, since lithium(I) recoveries are < 50 % by solar evaporation. The new techniques, such as solvent extraction, adsorption, nanofiltration, and electrochemical methods, aim to increase Li[I] production rates without relying on evaporation. In the extraction of lithium(I), solvent extraction offers 75 % to 99 % greater recovery rates.[73–77] However, large scale production would require large volumes of organic solvent, challenging its

recovery and suitable equipment selection.[21] Alternatively, lithium(I) extraction by adsorption would be a simple and attractive technique due to high lithium(I) selectivity (92-99 %) and adsorption capacity.[78–80] However, this technique in large-scale production can result in blockage of the ion channels reducing adsorbing capacity.[21] Additionally, the adsorbents may need frequent replacement making implementation complicated and potentially expensive. Nanofiltration for lithium(I) extraction is a simple method that can be conducted at room temperature, but lithium(I) recoveries have been reported to be relatively low, ranging from 12% to 55%.[81–83] Electrochemical methods for lithium(I) extraction offer great potential, avoiding the need for boron(III) removal processes and have low water (1.1 to 47.5 dm^3 s^{-1}) and electrical energy consumptions (0.001 to 0.013 kW h per mol Li^+).[84] Additionally, production times have been decreased to days and even hours. For example, lithium(I) in brine can be recovered selectively by electrochemical deintercalation/ intercalation system ($LiFePO_4/FePO_4$ EDI system), during which the Mg^{2+}, Ca^{2+}, SO_4^{2-} and $B_4O_7^{2-}$ removal rates were above 94 %.[85] In addition, $LiMn_2O_4/Li_{1-x}Mn_2O_4$ (LMO) electrochemical system with porous electrodes is also a promising method, which can recover lithium(I) directly from brine at a high rate and low specific electrical energy consumption.[86]

Overall, all those methods mentioned above offer distinct advantages and challenges in lithium(I) extraction, highlighting the necessity for comprehensive evaluation and consideration of factors such as recovery efficiency, environmental impact, operational feasibility, and cost benefit analysis in large-scale production scenarios.

3.4 Limitations and future perspectives

Although a detailed LCA of Li_2CO_3 production has been developed, it still has some limitations and shortcomings. Specifically, the waste management model was simplified; rectangular cuboid units were employed based on the methods of USEPA,[62] whereas waste piles often have conical or trapezoidal shapes in reality. These differences can affect the thickness of the accumulated fresh waste layer and further influence infiltration rates. Therefore, a more careful evaluation of the model parameters for real cases is required for an in-depth investigation of waste management. For water scarcity analysis, the water scarcity factor used is the Chilean average value. However, it is essential to obtain the latest water scarcity factor specific to the production site at the core of the Atacama Desert for a more detailed analysis at the regional level.

In recent years, several coal-fired power stations have been decommissioned in Chile and replaced with solar and wind energy generation. This change is expected to make the future electrical grid mix in Chile cleaner, and less carbon intensive. Therefore, it is reasonable to explore the environmental impact of Chile energy transition on lithium(I) production in the future. A comprehensive LCA study can be conducted of alternative methods of lithium(I) extraction from brine to compare with conventional evaporative techniques. This analysis can help to evaluate the environmental impacts, water resource

consumption, production output, duration, and economic benefits of each method, providing comprehensive guidance for lithium(I) production.

4. Conclusions

An up-to-date and more detailed LCI model has been established, based on chemical stoichiometry calculations, parameter modelling, and existing literature, technical reports, and the Ecoinvent database. This model involved optimisation through simulations, as well as calculations for every step of the process, including recycling. Due to the varying regional characteristics of brine production in each salar, and distinct freshwater resources surrounding different brine extraction sites, investigation of individual salars characteristics and extraction processes is considered necessary. Simulations of the northern Chile electricity grid mix, still dominated by fossil fuels, has helped produce more accurate results that are regionally specific. For waste management, although the accumulation of waste generated during Li carbonate production may not have had a significant impact on infiltration, still it is shown to result in occupation of significant land areas.

Detailed and complete analysis of 13 life cycle environmental impacts of this Li^I extraction process has predicted relatively low GWP (5.82 kg CO_2 (kg Li_2CO_3)$^{-1}$) and other impacts, but relatively high TETP (24.57 kg 1,4-DB eq. (kg Li_2CO_3)$^{-1}$) due to NaOH production. Considering water issues, three scenarios for the evaporation process have been simulated, adjusted, and compared to analyse the water balance results. Although the water footprint of the process was shown not to have been significant (0.29 m^3 (kg Li_2CO_3)$^{-1}$ to 0.92 m^3 (kg Li_2CO_3)$^{-1}$), it is crucial to note that this water has been extracted and pumped from an underground resource that is scarce in an extremely arid region. Therefore, the WSF of this seemingly low water-consuming Li^I production process was predicted to be relatively high significant (23.12 m^3 world equiv. (kg Li_2CO_3)$^{-1}$ to 74.55 m^3 world equiv. (kg Li_2CO_3)$^{-1}$). In addition to those disadvantages, the time-consuming production also resulted in low predicted lithium(I) recoveries and recovery rates during the evaporation process.

The growing demand in the Li_2CO_3 market is encouraging the conception and development of novel lithium(I) recovery processes. Although many alternative solutions have been studied and even up-scaled, they have not specifically addressed the question of how the brine will be treated after lithium(I) recovery. Through our water balance analysis, a significant volume of water from the brine was predicted to be lost from the system by evaporation; in such an extremely arid area those losses should not be ignored but considered as a potential resource for recovery. The results provided important insights of the life cycle impacts of Li_2CO_3 production and associated industries and can help guide lithium(I) production activities. Additionally, the results offer a scientific basis for environmental management in arid and similar regions.

Author Contributions

Zijing He: Conceptualisation, Methodology, Software, Investigation, formal analysis, Writing – original draft. **Anna Korre:** Conceptualisation, Supervision, Methodology, Writing – review & editing. **Geoff Kelsall:** Supervision, Writing – review & editing. **Zhenggang Nie:** Methodology. **Melanie Colet:** Methodology, Input data.

Conflicts of interest

There are no conflicts to declare.

List of symbol definitions and units

Symbol	Definition	Units
α	Albedo	/ 1
a	Area of holes in the geomembrane	m^2
a_U	Wind function coefficient	/ 1
D_{clog}	Thickness of clogged soil layer	m
D_{fc}	Thickness of consolidated sediment layer	m
D_{liner}	Thickness of consolidated sediment layer	m
E_a	Annual evaporation	mm a^{-1}
E_O	Corrected evaporation rate	mm day^{-1}
E_{PEN}	Calculated evaporation rate using Penman equation	mm day^{-1}
E_t	Recorded evaporation rate in the class A pan or calculations	mm day^{-1}
FC	Field capacity	vol vol^{-1}
h	Head of liquid on top of geomembrane	m
H_p	Pond depth of wastewater in the surface impoundment	m
i	Rank of month	/ 1
I	Average infiltration rate	m s^{-1}
I_a	Annual water infiltration	mm a^{-1}
K_{clog}	Saturated hydraulic conductivity of clogged soil	m s^{-1}
K_{fc}	Saturated hydraulic conductivity of consolidated sediment	m s^{-1}
K_{liner}	Saturated hydraulic conductivity of liner	m s^{-1}
K_e	Pond coefficient	/ 1
K_s	Hydraulic conductivity of the low-permeability soil underlying the geomembrane	m s^{-1}
K_S	Salinity reduction coefficient	/ 1
n	Bright sunshine hours per day	h
N	Maximum possible daylight duration	h
P_a	Annual precipitation	mm a^{-1}
Q	Steady-state rate of leakage through holes in composite liner	m^3 s^{-1}
RH	Relative humidity	%
R_A	Extraterrestrial irradiance	MJ m^{-2} day^{-1}
R_S	Solar irradiance	MJ m^{-2} day^{-1}
S	Footprint of the surface impoundment	m^2
S_i	Solid input	kg (kg Li_2CO_3)$^{-1}$
S_o	Solid output	kg (kg Li_2CO_3)$^{-1}$
T	Average temperature	°C
T_a	Thickness of the fresh waste layer accumulated	mm a^{-1}
u	Wind speed	m s^{-1}
W	Initial water content of the fresh waste	vol vol^{-1}

W_{ei}	External water input	kg (kg Li$_2$CO$_3$)$^{-1}$
W_{ii}	Internal water input	kg (kg Li$_2$CO$_3$)$^{-1}$
W_o	Water output	kg (kg Li$_2$CO$_3$)$^{-1}$
W_r	Recycled water	kg (kg Li$_2$CO$_3$)$^{-1}$
W_w	Wastewater	kg (kg Li$_2$CO$_3$)$^{-1}$
$\emptyset$	Latitude of the site	Rad
ρ	Leak density	holes m^{-2}

Abbreviations

EDI	Electrochemical Deintercalation/Intercalation
FDP	Fossil Depletion Potential
FEP	Freshwater Eutrophication Potential
FETP	Freshwater Ecotoxicity Potential
FPMFP	Fine Particulate Matter Formation Potential
GWP	Global Warming Potential
HTP	Human Toxicity Potential, cancer
LCA	Life Cycle Assessment
LCI	Life Cycle Inventory
LIB	Lithium-ion Battery
LMO	LiMn$_2$O$_4$/Li$_{1-x}$Mn$_2$O$_4$
MDP	Metal Depletion Potential
MEP	Marine Eutrophication Potential
METP	Marine Ecotoxicity Potential
POFP	Photochemical Oxidant Formation Potential, human health
SING	Sistema Interconectado del Norte Grande
SODP	Stratospheric Ozone Depletion Potential
SQM	Sociedad Química y Minera
TAP	Terrestrial Acidification Potential
TETP	Terrestrial Ecotoxicity Potential
WF	Water Footprint
WSF	Water Scarcity Footprint

Acknowledgements

References

1 U.S. Geological Survey, *Mineral commodity summaries 2024*, 2024.

2 International Energy Agency, *Net Zero Roadmap: A Global Pathway to Keep the 1.5 °C Goal in Reach*, 2023.

3 International Energy Agency, Global EV Outlook 2023, https://www.iea.org/reports/global-ev-outlook-2023/executive-summary, (accessed 1 April 2024).

4 B. W. Jaskula, *2018 Minerals Yearbook Lithium [Advance Release]*, U.S. Department of the Interior, U.S. Geological Survey, 2020.

5 H. Vikström, S. Davidsson and M. Höök, *Applied Energy*, 2013, **110**, 252–266.

6 C. Grosjean, P. H. Miranda, M. Perrin and P. Poggi, *Renewable and Sustainable Energy Reviews*, 2012, **16**, 1735–1744.

7 M. E. Q. Pilson, *An Introduction to the Chemistry of the Sea*, Cambridge University Press, 2012.

8 A. Shahmansouri, J. Min, L. Jin and C. Bellona, *Journal of Cleaner Production*, 2015, **100**, 4–16.

9 S. E. Kesler, P. W. Gruber, P. A. Medina, G. A. Keoleian, M. P. Everson and T. J. Wallington, *Ore Geology Reviews*, 2012, **48**, 55–69.

10 A. Seip, S. Safari, D. M. Pickup, A. V. Chadwick, S. Ramos, C. A. Velasco, J. M. Cerrato and D. S. Alessi, *Chemical Engineering Journal*, 2021, **426**, 130713.

11 A. Kumar, H. Fukuda, T. A. Hatton and J. H. V. Lienhard, *ACS Energy Lett.*, 2019, **4**, 1471–1474.

12 M. Figueira, D. Rodríguez-Jiménez, J. López, M. Reig, J. L. Cortina and C. Valderrama, *Desalination*, 2023, **549**, 116321.

13 S. Kim, J. Kim, S. Kim, J. Lee and J. Yoon, *Environ. Sci.: Water Res. Technol.*, 2018, **4**, 175–182.

14 V. Devda, K. Chaudhary, S. Varjani, B. Pathak, A. K. Patel, R. R. Singhania, M. J. Taherzadeh, H. H. Ngo, J. W. C. Wong, W. Guo and P. Chaturvedi, *Bioengineered*, 2021, **12**, 4697–4718.

15 N. A. A. Qasem, R. H. Mohammed and D. U. Lawal, *npj Clean Water*, 2021, **4**, 1–15.

16 A. Siekierka, M. Bryjak, A. Razmjou, W. Kujawski, A. N. Nikoloski and L. F. Dumée, *Membranes*, 2022, **12**, 343.

17 V. Flexer, C. F. Baspineiro and C. I. Galli, *Science of The Total Environment*, 2018, **639**, 1188–1204.

18 B. Swain, *Separation and Purification Technology*, 2017, **172**, 388–403.

19 L. Talens Peiró, G. Villalba Méndez and R. U. Ayres, *JOM*, 2013, **65**, 986–996.

20 D. E. Garrett, *Handbook of Lithium and Natural Calcium Chloride*, 2004.

21 J. F. Song, L. D. Nghiem, X.-M. Li and T. He, *Environ. Sci.: Water Res. Technol.*, 2017, **3**, 593–597.

22 C. Shi, Y. Jing and Y. Jia, *Journal of Molecular Liquids*, 2016, **215**, 640–646.

23 R. N. Hader, R. L. Nielsen and M. G. Herre, *Ind. Eng. Chem.*, 1951, **43**, 2636–2646.

24 M. Grágeda, A. González, W. Alavia and S. Ushak, *Energy*, 2015, **89**, 667–677.

25 V. T. Nguyen, C. Deferm, W. Caytan, S. Riaño, P. T. Jones and K. Binnemans, *J. Sustain. Metall.*, 2023, **9**, 107–122.

26 L. A.-W. Ellingsen, G. Majeau-Bettez, B. Singh, A. K. Srivastava, L. O. Valøen and A. H. Strømman, *Journal of Industrial Ecology*, 2014, **18**, 113–124.

27 E. Kallitsis, A. Korre, G. Kelsall, M. Kupfersberger and Z. Nie, *Journal of Cleaner Production*, 2020, **254**, 120067.

28 A. Stamp, D. J. Lang and P. A. Wäger, *Journal of Cleaner Production*, 2012, **23**, 104–112.

29 J. C. Kelly, M. Wang, Q. Dai and O. Winjobi, *Resources, Conservation and Recycling*, 2021, **174**, 105762.

30 Ministerio de Energia, *Anuario Estadístico de Energía año 2022*, 2020.

31 M. Chordia, S. Wickerts, A. Nordelöf and R. Arvidsson, *Resources, Conservation and Recycling*, 2022, **187**, 106634.

32 S. Khakmardan, M. Rolinck, F. Cerdas, C. Herrmann, D. Giurco, R. Crawford and W. Li, *Procedia CIRP*, 2023, **116**, 606–611.

33 V. Schenker, C. Oberschelp and S. Pfister, *Resources, Conservation and Recycling*, 2022, **187**, 106611.

34 A. C. Schomberg, S. Bringezu and M. Flörke, *Commun Earth Environ*, 2021, **2**, 1–10.

35 A.-M. Boulay, J. Bare, L. Benini, M. Berger, M. J. Lathuillière, A. Manzardo, M. Margni, M. Motoshita, M. Núñez, A. V. Pastor, B. Ridoutt, T. Oki, S. Worbe and S. Pfister, *Int J Life Cycle Assess*, 2018, **23**, 368–378.

36 Ecoinvent Association, Ecoinvent Database 3.9.1 https://ecoinvent.org/ 2024.

37 Aspen Tech, Aspen Plus https://www.aspentech.com/en/products/engineering/aspen-plus 2024.

38 Sphera Solutions, Life Cycle Assessment (LCA) Software https://about.sphera.com/ps 2023.

39 The International Organization for Standardization, *ISO 14040: 2006a Environmental Management-Life Cycle Assessment-Principles and Framework*, 2006a.

40 U.S. Patent, 5,993,759, 1999.

41 Sociedad Química y Minera de Chile, *Technical Report Summary Operation Report Salar de Atacama*, Av. Las Condes 11.700, Vitacura. Santiago, Chile, 2022.

42 T. Tran and V. T. Luong, in *Lithium Process Chemistry*, Elsevier, 2015, pp. 81–124.

43 J. D. Valiantzas, *Journal of Hydrology*, 2006, **331**, 690–702.

44 Sociedad Química y Minera de Chile, SQM monitor en línea, https://www.sqmsenlinea.com/meteorology/232, (accessed 3 April 2024).

45 Economic Charge Dispatch Center of the SING, The Chile CDED-SING, http://cdec2.cdec-sing.cl/pls/portal/cdec.pck_web_coord_elec.sp_pagina?p_id=5197, (accessed 1 April 2024).

46 Dirección General De Aeronáutica Civil and Dirección Meteorológica de Chile, Servicios Climáticos, https://climatologia.meteochile.gob.cl/application/requerimiento/producto/RE1011, (accessed 3 April 2024).

47 S. K. Kampf, S. W. Tyler, C. A. Ortiz, J. F. Muñoz and P. L. Adkins, *Journal of Hydrology*, 2005, **310**, 236–252.

48 W. Zhu, W. Xu, D. Liu, L. He, X. Liu and Z. Zhao, *Electrochimica Acta*, 2024, **475**, 143519.

49 F. Habashi, *Handbook of extractive metallurgy*, Wiley-VCH, 1997.

50 J. F. Muñoz-Pardo, C. A. Ortiz-Astete, L. Mardones-Pérez and P. de Vidts-Sabelle, *Tecnología y ciencias del agua*, 2004, **19**, 69–81.

51 T. A. Newson and M. Fahey, *Engineering Geology*, 2003, **70**, 217–233.

52 Y. Fujiyasil, PhD Thesis, The University of Western Australia, 1997.

53 T. A. Newson, Y. Fujiyasu and M. Fahey, *Proceedings of the Fourteenth International Conference on Soil Mechanics and Foundation Engineering*, 1997, **3**, 1973–1978.

54 L. Mardones, *El litio, un nuevo recurso para Chile*, 1986, 181–216.

55 F. Ide, PhD Thesis, Universidad de Chile, 1978.

56 Sociedad Química y Minera de Chile, Fresh water and brine: why they are different, https://www.sustainablelithium.com/what/, (accessed 5 February 2024).

57 J. S. Gutiérrez, J. N. Moore, J. P. Donnelly, C. Dorador, J. G. Navedo and N. R. Senner, *Proceedings of the Royal Society B: Biological Sciences*, 2022, **289**, 20212388.

58 W. Liu, D. B. Agusdinata and S. W. Myint, *International Journal of Applied Earth Observation and Geoinformation*, 2019, **80**, 145–156.

59 J. C. Molinare, PhD Thesis, Imperial College London, 2014.

60 M. M. Aldaya, A. K. Chapagain, A. Y. Hoekstra and M. M. Mekonnen, 2012.

61 Vicepresidencia Operaciones Potasio Litio, *Undécimo Informe de Extracción Anual de Salmuera de las Operaciones en el Salar de Atacama*, 2019.

62 U.S. Environmental Protection Agency, *EPA's Composite Model for Leachate Migration with Transformation Products (EPACMTP) Technical Background Document*, 2023.

63 U.S. Environmental Protection Agency, *EPA's Composite Model for Leachate Migration with Transformation Products (EPACMTP) Parameters/Data Background Document*, 2023.

64 J. Finch and A. Calver, *Methods for the quantification of evaporation from lakes*, 2008.

65 M. A. Marazuela, E. Vázquez-Suñé, C. Ayora and A. García-Gil, *Science of The Total Environment*, 2020, **703**, 135605.

66 W. Liu and D. B. Agusdinata, *The Extractive Industries and Society*, 2021, **8**, 100927.

67 Ministerio de Energía, Proyecciones Eléctricas, https://energia.gob.cl/pelp/proyecciones-electricas, (accessed 5 August 2024).

68 Sociedad Química y Minera de Chile, *Sustainability of lithium production in Chile*, 2021.

69 Global Corporate Website, Saving energy in chlorine production, https://www.covestro.com/en/sustainability/flagship-solutions/oxygen-depolarized-cathode, (accessed 17 April 2024).

70 I. Garcia-Herrero, M. Margallo, R. Onandía, R. Aldaco and A. Irabien, *Sustainable Production and Consumption*, 2017, **12**, 44–58.

71 I. Garcia-Herrero, M. Margallo, R. Onandía, R. Aldaco and A. Irabien, *Science of The Total Environment*, 2017, **580**, 147–157.

72 J. Wu, B. Li and J. Lu, *Clean Techn Environ Policy*, 2021, **23**, 1981–1991.

73 T. Sekimoto, S. Nishihama and K. Yoshizuka, *Solvent Extraction Research and Development, Japan*, 2018, **25**, 117–123.

74 D. Shi, B. Cui, L. Li, X. Peng, L. Zhang and Y. Zhang, *Separation and Purification Technology*, 2019, **211**, 303–309.

75 L. Zhang, L. Li, D. Shi, X. Peng, F. Song, F. Nie and W. Han, *Hydrometallurgy*, 2018, **175**, 35–42.

76 W. Xiang, S. Liang, Z. Zhou, W. Qin and W. Fei, *Hydrometallurgy*, 2017, **171**, 27–32.

77 L. Ji, Y. Hu, L. Li, D. Shi, J. Li, F. Nie, F. Song, Z. Zeng, W. Sun and Z. Liu, *Hydrometallurgy*, 2016, **162**, 71–78.

78 S. Wang, P. Li, X. Zhang, S. Zheng and Y. Zhang, *Hydrometallurgy*, 2017, **174**, 21–28.

79 J.-L. Xiao, S.-Y. Sun, X. Song, P. Li and J.-G. Yu, *Chemical Engineering Journal*, 2015, **279**, 659–666.

80 X. Shi, D. Zhou, Z. Zhang, L. Yu, H. Xu, B. Chen and X. Yang, *Hydrometallurgy*, 2011, **110**, 99–106.

81 Y. Li, Y. Zhao, H. Wang and M. Wang, *Desalination*, 2019, **468**, 114081.

82 A. Somrani, A. H. Hamzaoui and M. Pontie, *Desalination*, 2013, **317**, 184–192.

83 X. Wen, P. Ma, C. Zhu, Q. He and X. Deng, *Separation and Purification Technology*, 2006, **49**, 230–236.

84 J. A. A. Dietz, J. T. V. Valero, M. A. C. Lagrille and G. E. M. Naranjo, Undergraduate Thesis, Universidad de Chile, 2021.

85 D. Liu, Z. Zhao, W. Xu, J. Xiong and L. He, *Desalination*, 2021, **519**, 115302.

86 D. Liu, W. Xu, J. Xiong, L. He and Z. Zhao, *Separation and Purification Technology*, 2021, **270**, 118809.

The data supporting this article have been included as part of the Supplementary Information.